XVI CONGRESSO BRASILEIRO DE ENGENHARIA MECÂNICA
16th BRAZILIAN CONGRESS OF MECHANICAL ENGINEERING

COMPARISON OF LOAD INTERACTION MODELS IN FATIGUE CRACK PROPAGATION

Marco Antonio Meggiolaro
Pontifícia Universidade Católica do Rio de Janeiro (PUC-Rio) - Dept. Eng. Mecânica
Rua Marquês de São Vicente, 225 Gávea, Rio de Janeiro, RJ 22453-900
meggi@mec.puc-rio.br

Jaime Tupiassú Pinho de Castro
Pontifícia Universidade Católica do Rio de Janeiro (PUC-Rio) - Dept. Eng. Mecânica
Rua Marquês de São Vicente, 225 Gávea, Rio de Janeiro, RJ 22453-900
jtcastro@mec.puc-rio.br

Abstract. *Several mathematical models have been developed to account for load interaction effects in mode I fatigue crack propagation, based on Elber's crack closure idea. Elber described, with the aid of a physical model, the connection between load sequence, plastic deformation and crack propagation, assuming that crack growth cannot take place under cyclic loads until the crack is fully opened. Since overloads induce compressive stress states ahead of the crack tip after the load is removed, a reduction in crack propagation under a smaller succeeding load cycle is expected. Such retardation mechanisms are only considered within the overload-induced plastic zone situated in front of the crack tip. In this paper a review of the main load interaction models, such as the Wheeler and the Generalized Willenborg models, is presented. Modifications to the traditional retardation models are proposed to better model such effects as crack arrest and reduction in crack retardation due to underloads. The traditional models and the proposed modifications have been implemented on a software called ViDa, developed to automate the fatigue dimensioning process by all the traditional methods used in mechanical design. Using this software, the presented load interaction models and the proposed modifications are compared with experimental results from the literature for various load spectra.*

Keywords: *fatigue, crack propagation, sequence effects*

1. Introduction

It is well known that load cycle interactions can have a very significant effect in the prediction of fatigue crack growth. There is a vast literature proving that tensile overloads, when applied over a loading whose amplitude otherwise stays constant, can retard or even arrest the subsequent crack growth (Broek, 1988; Suresh, 1998; Castro and Meggiolaro, 2001). Neglecting these effects in fatigue life calculations under complex loading can completely invalidate the predictions.

However, the generation of a universal algorithm to quantify these effects for design purposes is particularly difficult, due to the number and to the complexity of the mechanisms involved in fatigue crack retardation, among them: plasticity-induced crack closure; blunting and/or bifurcation of the crack tip; residual stresses and/or strains; strain-hardening and/or strain induced phase transformation; crack face roughness; and oxidation of the crack faces. The detailed discussion of this complex phenomenology is considered beyond the scope of this work, but a revision of the phenomenological problem can be found in Suresh (1998).

Besides, depending on the case, several of these mechanisms may act concomitantly or competitively, as a function of factors such as size of the crack; microstructure of the material; dominant stress state; and environment. Moreover, the relative importance of the several mechanisms can vary from case to case, and there is so far no universally accepted single equation capable of describing the whole problem. Therefore, from the fatigue designer's point of view, it must necessarily be treated in the most reasonably simplified way.

On the other hand, the principal characteristic of fatigue cracks is to propagate cutting a material that has already been deformed by the plastic zone that always accompanies their tips. Therefore, fatigue crack faces are always embedded in an envelope of (plastic) residual strains and, consequently, they compress their faces when completely discharged, and open alleviating in a progressive way the (compressive) load transmitted through them.

In this work, a review of plasticity induced crack closure is presented, along with the models proposed to quantify its effect on the subsequent crack growth rate. A taxonomy of load interaction models based on the crack closure idea is introduced, and improvements to the traditional retardation models are proposed to better model crack arrest and crack acceleration after compressive underloads. The models are compared using a general-purpose fatigue design software named `ViDa` . A review of the crack closure models is presented next.

2. Crack closure

Elber (1971) discovered that fatigue cracks opened gradually, remaining partially closed for loads substantially higher than zero. This was attributed to the compressive loads transmitted through the faces of an unloaded fatigue crack, caused by the plastic strains surrounding it, a phenomenon termed ***plasticity-induced fatigue crack closure***.

Elber was one of the first to attempt to describe, with the aid of a physical model, the connection between load sequence, plastic deformation (by way of crack closure) and crack growth rate. He assumed that crack expansion cannot take place under cyclic loads until the fatigue crack is fully opened. According to him, only after the load completely opened the crack at a stress intensity factor $\mathbf{K_{op} > 0}$, would the crack tip be stressed. Therefore, the bigger the $\mathbf{K_{op}}$, the less would be the ***effective*** stress intensity range $\mathbf{\Delta K_{eff} = K_{max} - K_{op}}$, and this $\mathbf{\Delta K_{eff}}$ instead of $\mathbf{\Delta K = K_{max} - K_{min}}$ would be the fatigue crack propagation rate controlling parameter.

Based on experiments on 2024-T3 aluminum, Elber proposed a modification to the Paris growth law by using this effective stress-intensity range to calculate the crack propagation under constant amplitude loads, taking into account the crack closure concept:

$$\frac{da}{dN} = A \cdot (K_{max} - K_{op})^m = A \cdot (\Delta K_{eff})^m \tag{1}$$

where **A** and **m** are the experimental growth rate constants. Note that $\mathbf{\Delta K = (1 - R) \cdot K_{max}}$, and the fatigue crack growth rate **da/dN** tends to **0** when $\mathbf{\Delta K}$ tends to $\mathbf{\Delta K_{th}}$, the propagation threshold. This implies that $\mathbf{\Delta K_{th} = (1 - R) \cdot K_{op}}$ when closure is the only crack arrest mechanism, and that $\mathbf{\Delta K_{eff}}$ is dependent on the stress ratio $\mathbf{R = K_{min}/K_{max}}$:

$$\frac{da}{dN} = A \cdot (\Delta K_{eff})^m = A \cdot \left(\frac{(K_{max} - K_{op}) \cdot (1 - R)}{1 - R} \right)^m = A \cdot \left(\frac{\Delta K - \Delta K_{th}}{1 - R} \right)^m \tag{2}$$

The threshold stress intensity factor range used in this model can be determined for any stress ratio $\mathbf{R > 0}$ by:

$$\Delta K_{th} = (4/\pi) \cdot \Delta K_0 \cdot \arctan(1 - R) \tag{3}$$

where $\mathbf{\Delta K_0}$ is the crack propagation threshold value of the stress-intensity factor range obtained from $\mathbf{R = 0}$ constant amplitude tests (Forman et al., 1992).

Newman (1984) found that crack closure does not only depend on **R**, as Elber found, but is also dependent on the maximum stress level $\mathbf{\sigma_{max}}$. He proposed an equation for the crack opening function **f**, which includes the effects of the ratio between the maximum stress $\mathbf{\sigma_{max}}$ and the material flow strength $\mathbf{S_{fl}}$ (defined as the average between the material yielding and ultimate strengths, $\mathbf{S_{fl} = (S_Y + S_U)/2}$), and of a plane stress/strain constraint factor α, with values ranging from $\alpha = 1$ for plane stress to $\alpha = 3$ for plane strain:

$$f = \frac{K_{op}}{K_{max}} = \begin{cases} \max(R, A_0 + A_1 R + A_2 R^2 + A_3 R^3), & R \geq 0 \\ A_0 + A_1 R, & -2 \leq R < 0 \end{cases} \tag{4}$$

where the polynomial coefficients are given by:

$$\begin{cases} A_0 = (0.825 - 0.34\alpha + 0.05\alpha^2) \cdot [\cos(\pi\sigma_{max} / 2S_{fl})]^{1/\alpha} \\ A_1 = (0.415 - 0.071\alpha) \cdot \sigma_{max} / S_{fl} \\ A_2 = 1 - A_0 - A_1 - A_3 \\ A_3 = 2A_0 + A_1 - 1 \end{cases} \tag{5}$$

Increasing values of the maximum stress cause reduction in the Newman closure function, resulting in reduction in crack retardation. From the definition of the Newman's closure function **f**, the effective stress intensity range $\mathbf{\Delta K_{eff} = K_{max} - K_{op}}$ can be rewritten as

$$\Delta K_{eff} = (1 - f) \cdot K_{max} = \frac{1 - f}{1 - R} \Delta K \tag{6}$$

Assuming that the fatigue crack growth rate is ***controlled*** by $\mathbf{\Delta K_{eff}}$ instead of by $\mathbf{\Delta K}$ (and, therefore, that closure is the only mechanism which affects the propagation process), the need for taking into account crack closure effects when experimentally obtaining **da/dN** equation constants must be stressed. Consider, for instance, the effective stress intensity range $\mathbf{\Delta K_{eff}}$ predicted by Newman for the ***plane stress*** case with $\mathbf{R = 0}$, using Eqs. (4-6). In this case, $\mathbf{\Delta K_{eff}}$ is approximately equal to **half** the value of $\mathbf{\Delta K}$. This means that the **da/dN** curves experimentally fitted to $\mathbf{\Delta K}$ values ***without*** considering the crack closure effect would be actually correlating the measured **da/dN** rates with ***twice*** the actual (effective) stress intensity range acting on the crack tip. On the other hand, **da/dN** curves obtained in the same way ($\mathbf{R = 0}$) under ***plane strain*** conditions would be actually correlating **da/dN** with **4/3** (and ***not twice***) of the effective stress intensity range. Therefore, one could not indiscriminately use crack growth equation constants obtained under a certain stress condition (e.g. plane stress) to predict crack growth under a different state (e.g. plane strain), even under the same stress ratio **R**.

E.g., if a Paris **da/dN** vs. **ΔK** equation with exponent $\mathbf{m = 3.0}$, measured under plane stress conditions and $\mathbf{R = 0}$, is used to predict crack propagation under plane strain, the predicted crack growth rate would be $\mathbf{[(4/3)/2]^m \approx 0.3}$ times the actual rate, a ***non-conservative error of*** **70%**. In this case, it would be necessary to convert the measured crack growth constants associated with one stress condition to the other using appropriate crack closure functions, to avoid this error. Another approach would be to use in the predictions **da/dN** vs. **ΔK** equations that already have embedded the closure functions.

This alarming result implies that the usual practice of plotting **da/dN** vs. **ΔK** instead of $\mathbf{\Delta K_{eff}}$ would be highly inappropriate, because **da/dN** would also be a strong function of the specimen thickness **t**, which controls the dominant stress state at the crack tip. Assuming that the classical ASTM E399 requirements for validating a $\mathbf{K_{IC}}$ toughness test can also be used in fatigue crack growth, plane strain conditions would apply if $\mathbf{t > 2.5(K_{max}/S_Y)^2}$. Therefore, one could expect quite different **da/dN** fatigue crack growth rates when thin or thick specimens were tested under the same **ΔK**. But fatigue designers normally do not consider **t** as such an important parameter in crack growth calculations.

In any way, it is very important to emphasize that crack closure is by no means the only mechanism that can induce crack retardation. For example, Castro and Parks (1982) showed that, under dominant plane strain conditions, overload induced fatigue crack retardation or stop can occur while $\mathbf{\Delta K_{eff}}$ ***increases***. It was found that just after the overload the opening load ***decreased***, a behavior completely incompatible with Elber-type crack closure. The principal retardation mechanism in those cases was bifurcation of the crack tip.

Even though the above example shows the crack closure concept in a different light, most load interaction models are, directly or indirectly, based on Elber's original idea. This implicates in the supposition that the main retardation mechanism is caused by plasticity induced crack closure: in these cases, the opening load $\mathbf{K_{op}}$ should ***increase*** due to the plastic zone ahead of the crack tip, ***reducing*** the $\mathbf{\Delta K_{eff}}$ and delaying the crack growth.

However, the equations presented in this section are derived from experimental data or finite-element predictions for ***constant-amplitude*** fatigue tests. As such they can account for closure effects in ***constant*** amplitude fatigue data (by collapsing **da/dN** vs. **ΔK** curves for multiple **R** values), but they ***cannot*** account for stress-interaction effects such as growth rate retardation or acceleration ***after*** overloads or underloads. To recognize load interaction effects, it is in general necessary to compute the overload-induced plastic zone size and compare it with the (embedded) current plastic zone. The next section presents analytical models to account for such load interaction effects.

3. Load interaction models

Several mathematical models have been developed to account for load interaction effects in fatigue crack propagation based on Elber's crack closure idea. In these models, the retardation mechanism is considered to act only within the overload-induced plastic zone situated in front of the crack tip. The size of this overload plastic zone being (considerably) greater than the size of the plastic zone induced by subsequent load cycles, an increased compressive stress state would be set up inside that region, which would be then the main contributing factor for reducing the crack propagation rate under smaller succeeding load cycles.

Perhaps the best-known fatigue crack growth retardation models are those developed by Wheeler (1972) and by Willenborg et al. (1971). Both use the same idea to decide whether the crack is retarded or not: under variable loading, fatigue crack growth retardation is predicted when the plastic zone of the i-th load event $\mathbf{Z_i}$ is embedded within the plastic zone $\mathbf{Z_{ol}}$ induced by a previous overload, and it is assumed dependent on the distance from the border of $\mathbf{Z_{ol}}$ to the tip of the i-th crack plastic zone $\mathbf{Z_i}$, see Fig. (1).

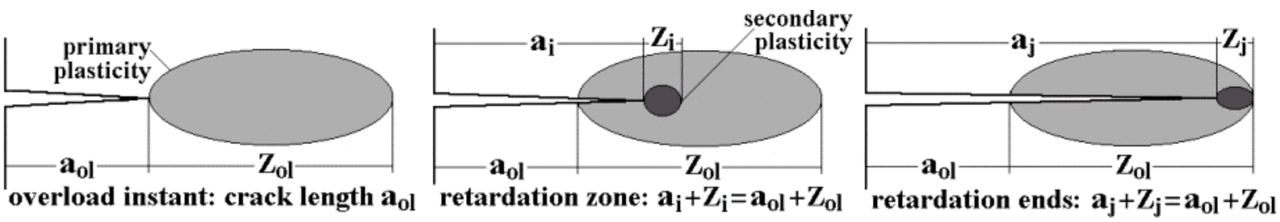

Figure 1. Yield zone crack growth retardation region used by Wheeler and by Willenborg.

In Fig. (1), $\mathbf{a_{ol}}$ is the size of the crack when the overload occurs, and $\mathbf{a_i}$ is the (larger) crack size at the i-th load event, which occurs after the overload. According to both the Wheeler and the Willenborg models, load interaction effects would end when $\mathbf{a_{ol} + Z_{ol} = a_i + Z_i}$. Moreover, the magnitude of the retardation effect would be a function of $\mathbf{Z_i/(Z_{ol} + a_{ol} - a_i)}$, it would be maximum in the very first cycle after the overload, and it would steadily decrease as the crack progressively grew though the overload plastic zone.

This assumption may be mathematically convenient, but it is hard to physically justify. If the crack must enter the overload inflated plastic zone to be retarded, it does not seem reasonable to assume that the maximum retardation effect occurs in the very first cycle after it, when the crack barely crossed the $\mathbf{Z_{ol}}$ frontier. In fact, Von Euw et al. (1972)

obtained experimental results under ***plane stress*** conditions which support this view. Moreover, it must be emphasized again that plasticity induced crack closure is ***not*** the only important mechanism which can induce retardation effects.

The main difference between the Wheeler and Willenborg models is that the latter quantifies the retardation effect by reducing $\mathbf{K_{max}}$ and $\mathbf{K_{min}}$ acting on the crack tip, while Wheeler accounts it by direct reduction of the crack propagation rate **da/dN**. Based on this and other differences, the load interaction models presented in this paper are divided in 4 categories:

(i) **da/dN** models, such as the Wheeler model, which use retardation functions to directly reduce the calculated crack propagation rate **da/dN**;

(ii) **ΔK** models, which use retardation functions to reduce the stress intensity range **ΔK**;

(iii) $\mathbf{R_{eff}}$ models, such as the Willenborg model, which introduce an effective stress ratio $\mathbf{R_{eff}}$, calculated by reducing the maximum and minimum stress intensity factors $\mathbf{K_{max}}$ and $\mathbf{K_{min}}$ acting on the crack tip (however not necessarily changing the value of **ΔK**); and

(iv) $\mathbf{K_{op}}$ models, such as the strip yield model, which use estimates of the opening stress intensity factor $\mathbf{K_{op}}$ to directly account for Elber-type crack closure.

3.1. da/dN interaction models

The **da/dN** interaction models use retardation functions to directly reduce the calculated crack propagation rate **da/dN**. ***Wheeler*** (1972) is the most popular of such models. He introduced a crack-growth reduction factor, $\mathbf{C_r}$, bounded by zero and unity, which is calculated for each cycle and is used as a multiplying factor on the crack growth rate for each cycle. There is retardation as long as the current plastic zone is contained within a previously overload-induced plastic zone; this is the fundamental assumption of the yield zone models. The retardation is maximum just after the overload, and stops when the border of $\mathbf{Z_i}$ touches the border of $\mathbf{Z_{ol}}$, see Fig. (1).

Therefore, if $\mathbf{a_{ol}}$ and $\mathbf{a_i}$ are the crack sizes at the instant of the overload and at the (later) *i*-th cycle, and $\mathbf{(da/dN)_{ret,i}}$ and $\mathbf{(da/dN)_i}$ are the retarded and the corresponding non-retarded crack growth rate (at which the crack would be growing in the *i*-th cycle if the overload had not occurred), then, according to Wheeler:

$$\left(\frac{da}{dN}\right)_{ret,i} = \left(\frac{da}{dN}\right)_i \cdot C_r = \left(\frac{da}{dN}\right)_i \cdot \left(\frac{Z_i}{Z_{ol} + a_{ol} - a_i}\right)^{\beta}, \quad a_i + Z_i < a_{ol} + Z_{ol} \tag{7}$$

where **β** is an experimentally adjustable constant.

The exponent **β** is obtained by selecting the closest match among predicted crack growth curves (using several **β**-values) with an experimental curve obtained under spectrum loading. Wheeler found experimentally that the shaping exponent, **β**, was material dependent, having values of 1.43 for a steel and 3.4 for the titanium alloy Ti-6AL-4V. Broek (1988) suggests that other typical values for **β** are between 0 and 2. However, flight-by-flight crack propagation tests performed by Sippel et al. (1977) have shown that the exponent **β** is dependent not only on the material, but also on crack shape, stress level, as well as type of load spectrum. Therefore, the designer should be aware that life predictions based on limited amounts of supporting test data, or for spectra radically different from those for which the exponent **β** was derived, can lead to inaccurate and ***non-conservative*** results.

In summary, the selection of proper values for the Wheeler exponent **β** can yield reasonable crack-growth predictions when the (complex) loads have similar spectra. However, the Wheeler model cannot predict the phenomenon of crack ***arrest***. As $\mathbf{Z_i \approx (K_{max}/S_Y)^2}$, the lowest value of the predicted retardation factor happens immediately after the overload, and is equal to $\mathbf{(K_{max}/K_{ol})^{2\beta}}$, where $\mathbf{K_{max}}$ is the maximum stress intensity factor in the cycle just after the overload, and $\mathbf{K_{ol}}$ is the overload stress intensity factor. Therefore, the phenomenology of the load cycle interaction problem is not completely reproducible by the Wheeler model, since such retardation factor is always different than zero. To consider crack arrest, a modification of the Wheeler original model is presented next.

3.2. ΔK interaction models

The **ΔK** interaction models use retardation functions to directly reduce the value of the stress intensity range **ΔK**. Meggiolaro and Castro (1997) proposed a simple but effective modification to the original Wheeler model in order to predict both crack retardation and arrest. This approach, called the ***Modified Wheeler*** model, uses a Wheeler-like parameter to multiply **ΔK** instead of **da/dN** after the overload:

$$\Delta K_{ret}(a_i) = \Delta K(a_i) \cdot \left(\frac{Z_i}{Z_{ol} + a_{ol} - a_i}\right)^{\gamma}, \quad a_i + Z_i < a_{ol} + Z_{ol} \tag{8}$$

where $\mathbf{\Delta K_{ret}(a_i)}$ and $\mathbf{\Delta K(a_i)}$ are the values of the stress intensity ranges that would be acting at $\mathbf{a_i}$ with and without retardation due to the overload, and **γ** is an experimentally adjustable constant, in general different from the original Wheeler model exponent **β**. This simple modification can be used with any of the propagation rules that recognize $\mathbf{\Delta K_{th}}$

to predict both the retardation and the arrest of fatigue cracks after an overload (the arrest occurring if $\Delta K_{ret}(a_i) \le \Delta K_{th}$). In addition to the retarded stress intensity range ΔK_{ret}, the retarded stress ratio R_{ret} can also be calculated:

$$R_{ret}(a_i) = 1 - \Delta K_{ret}(a_i) / K_{max} \tag{9}$$

where K_{max} is the maximum load at the *i*-th cycle.

However, the Modified Wheeler model does not predict the reduction of retardation effects due to underloads subsequent to overload cycles, a phenomenon also referred to as crack acceleration (Suresh, 1998). An underload cycle occurs when its minimum value K_{min} is significantly smaller than the corresponding values of the previous or the subsequent cycles.

Chang et al. (1984) proposed the concept of an effective overload plastic zone to model crack acceleration. In Chang's crack acceleration concept, the overload plastic zone Z_{ol} is reduced to $(Z_{ol})_{ul}$ after a compressive underload, reducing the crack retardation effects by increasing the retardation parameter from Eqs. (7-8). Chang's acceleration concept was originally developed for the Willenborg model, considering that the compressive underload ***immediately*** follows the overload, but it may be adapted to the Wheeler and Modified Wheeler models using

$$(Z_{ol})_{ul} = (1+\overline{R}_{ul}) \cdot Z_{ol}, \text{ where } \overline{R}_{ul} = \max(R_{ul}, R^{-}) \tag{10}$$

where $R_{ul} < 0$ is the underload stress ratio σ_{ul}/σ_{ol}, σ_{ul} is the lowest underload stress after the most recent overload σ_{ol}, and R^{-} is a cutoff value for negative stress ratios (with $-1 < R^{-} < 0$ and, in general, $R^{-} = -0.5$).

To consider the crack acceleration effect due to underload stresses, an extension of the Modified Wheeler model, called ***Generalized Wheeler***, is proposed here. Based on Chang's crack acceleration concept, the Generalized Wheeler model calculates the reduced stress intensity range by:

$$\Delta K_{red} = \Delta K \cdot \left(\frac{Z_i}{(1+\alpha' \overline{R}_{ul})Z_{ol} + a_{ol} - a_i} \right)^{\gamma}, \quad a_i + Z_i < a_{ol} + Z_{ol} \tag{11}$$

where $\overline{R}_{ul}$ is defined in Equation (28), α' is a positive parameter to multiply $\overline{R}_{ul}$ to better model the influence of underload stresses on crack acceleration, and γ is the Modified Wheeler's exponent. This proposed model recognizes crack retardation and arrest due to overloads and crack acceleration (reduction in retardation) due to underloads. Furthermore, closure effects under constant amplitude loading can be easily considered in all ΔK interaction models by multiplying ΔK_{red} by $(1-f)/(1-R)$, where f is Newman's closure function from Eqs. (4-5). Another advantage of the Generalized Wheeler model is that it can be applied to ***any*** **da/dN** equation (preferably to one that recognizes ΔK_{th} to also model crack arrest), in contrast with the Willenborg model, which can only be applied to **da/dN** equations that explicitly model the stress ratio **R**, as explained below.

3.3. R_{eff} interaction models

In the R_{eff} models, an effective stress ratio R_{eff} is introduced, calculated by reducing the maximum and minimum stress intensity factors acting on the crack tip. The best-known R_{eff} model is the ***Willenborg*** (1971) model. As in the Wheeler model, the retardation for a given applied cycle depends on the loading and the extent of crack growth into the overload plastic zone. Willenborg et al. assumed that the maximum stress intensity factor K_{max} occurring at the current crack length a_i will be reduced by a residual stress intensity K_R^W. The value of K_{RW} is calculated, more or less arbitrarily, from the difference between the stress intensity required to produce a plastic zone that would reach the overload zone border (distant $Z_{ol} + a_{ol} - a_i$ from the current crack tip) and the current maximum stress intensity K_{max},

$$K_{RW} = K_{ol}\sqrt{(Z_{ol} + a_{ol} - a_i)/Z_{ol}} - K_{max} \tag{12}$$

where K_{ol} is the maximum stress intensity of the overload, Z_{ol} is the overload plastic zone size, and a_{ol} is the crack size at the ocurrence of the overload, see Fig. (1).

Willenborg et al. expect that the stress-intensity factor cycle, and therefore, its maximum and minimum levels K_{max} and K_{min}, are reduced by the same amount K_{RW}. Thus, since the range in stress-intensity factor ΔK is unchanged by the uniform reduction, the retardation effect is only sensed by the change in the effective stress ratio R_{eff} calculated by

$$R_{eff} = \frac{K_{eff,min}}{K_{eff,max}} = \frac{K_{min} - K_{RW}}{K_{max} - K_{RW}} \tag{13}$$

As a result, crack propagation rules that do not model explicitly the effects of the stress ratio **R** ***cannot*** be used with the Willenborg retardation model. For instance, if the Paris law is used for crack propagation, the Willenborg model will ***not*** predict crack retardation after overloads, since the value of ΔK remains unchanged (and thus the value of **da/dN** as well). This is a limitation of the original Willenborg formulation, not present in the Wheeler model.

Another problem in the original Willenborg model is the prediction that $K_{eff,max} = 0$ (and therefore crack arrest) immediately after an overload if $K_{ol} \geq 2\ K_{max}$. That is, if the overload is twice as large as (or larger than) the following loads, the Willenborg model implies that the crack arrests, independently of the material properties, stress level, or load spectrum.

To account for the observations of continuing crack propagation after overloads larger than a factor of two or more (i.e. shut-off ratios larger than 2), Gallagher (1974) generalized Willenborg's original development by introducing an empirical (spectra/material) constant into the calculations. In Gallagher's ***Generalized Willenborg*** model, a modified residual stress intensity $K_R = \Phi \cdot K_{RW}$ is used, instead of Willenborg's original K_{RW}, where Φ is given by

$$\Phi = \frac{1 - \Delta K_{th} / \Delta K}{R_{so} - 1} \tag{14}$$

and R_{so} is a constant defined as the overload (shut-off) ratio required to cause crack arrest. Using this constant it is possible to model shut-off ratios different than 2 for K_{ol}/K_{max}, compensating for this Willenborg's original model limitation. Typical values for R_{so} are 3.5 for steel and nickel alloys, and 2.3 for aluminum and titanium alloys. The value of the shut-off ratio R_{so} is not only material-dependent, but it is also affected by the stress level and the frequency of overload cycle occurrence. However, in the Generalized Willenborg model, no special consideration is given to multiple overloads or stress levels, and their effect is taken to be the same as that for a single overload. Also, this model cannot predict the observed reduction in crack retardation after underloads.

To account for the reduction of retardation effects due to compressive or even tensile underloads, a load interaction model termed ***Modified Generalized Willenborg*** (MGW) has been developed (Gallagher, 1974). As in the Generalized Willenborg (GW) model, the MGW model uses a residual stress intensity K_R to determine the effective maximum and minimum stress intensity factors due to a load interaction. In the MGW model, the effective maximum stress intensity factor $K_{eff,max}$ is calculated in the same way as in the GW model, however the effective minimum stress intensity factor $K_{eff,min}$ is modified to better model the influence of negative values of R_{eff}:

$$K_{eff,min} = \begin{cases} (K_{min} - K_R), \text{ if } K_{min} > K_R \\ 0, \text{ if } 0 < K_{min} \leq K_R \\ K_{min}, \text{ if } K_{min} \leq 0 \end{cases} \tag{15}$$

As seen in Eq. (15), the value of $K_{eff,min}$ is set to zero for positive K_{min} smaller than the residual stress intensity K_R, and the K_R correction on $K_{eff,min}$ is ignored for negative values of K_{min}. In these cases, both the values of $\Delta K_{eff} = K_{eff,max} - K_{eff,min}$ and R_{eff} are increased if compared to the Willenborg and GW models, resulting in **less** predicted retardation by the MGW than by the other two models. However, such reduction in retardation for small or negative values of K_{min} is only accounted ***at*** the underload event.

To account for reduction in retardation ***after*** an underload, the MGW model uses a different modifying parameter Φ for the value of K_{RW}. The new value of Φ, used to achieve the reduction in retardation, is defined in the MGW model as a function of the underload stress ratio R_{ul}, given by S_{ul} / S_{ol} (where S_{ul} is the lowest underload stress ***after*** the most recent overload S_{ol}),

$$\Phi = \begin{cases} \min\left(1, \dfrac{2.523 \cdot \Phi_0}{1 + 3.5 \cdot (0.25 - R_{ul})^{0.6}}\right), & \text{if } R_{ul} < 0.25 \\ 1.0, & \text{if } R_{ul} \geq 0.25 \end{cases} \tag{16}$$

where the parameter Φ_0 is the value of Φ for $R_{ul} = 0$. The material-dependent parameter Φ_0 can be determined by conducting a series of experimental spectrum tests, and its value ranges typically from 0.2 to 0.8. Note that the MGW model predicts reduction in retardation not only for compressive underloads, but also for ***tensile*** underloads with magnitudes up to 25% of the maximum overload stress ($R_{ul} \leq 0.25$).

Figure (2) shows a comparison of the Willenborg, GW, and MGW models, representing the calculated value of R_{eff} immediately after the overload (thus $a_i = a_{ol}$ and $K_{RW} = K_{ol} - K_{max}$) as a function of the overload ratio K_{ol}/K_{max} for various stress ratios **R**. In this plot, it is assumed that both GW's and MGW's modifying parameters Φ are equal to 0.3 (considering $\Delta K_{th}/\Delta K = 0.22$ for the current cycle and the estimate $R_{so} = 2.3$ for aluminiums for the GW, and $R_{ul} = 0$ and $\Phi_0 = 0.6$ for the MGW model).

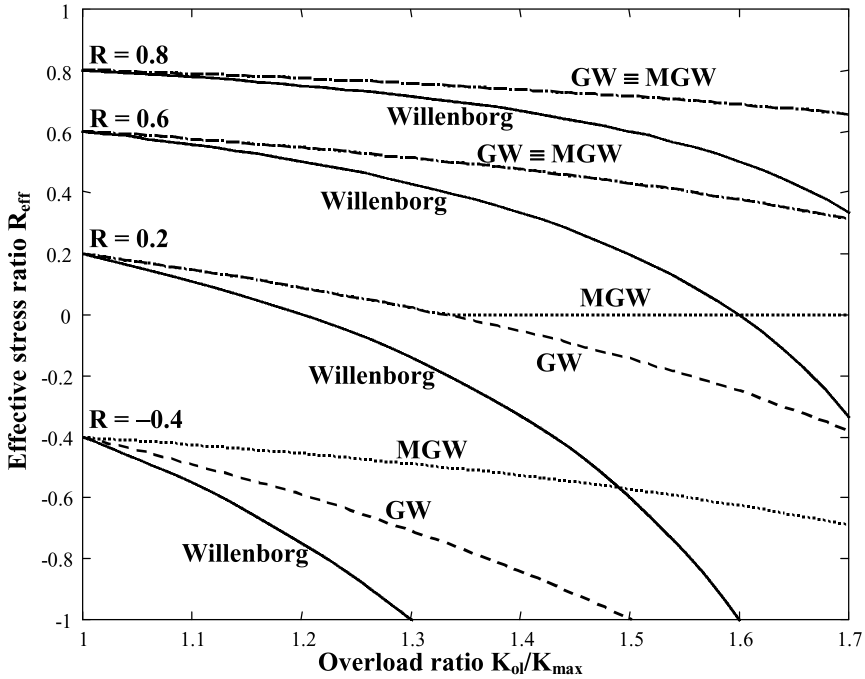

Figure 2. Influence of the overload ratio $\mathbf{K_{ol}/K_{max}}$ on the effective stress ratio $\mathbf{R_{eff}}$.

Note that in general the GW model predicts larger $\mathbf{R_{eff}}$ values (and thus ***less*** retardation) than Willenborg's original model. Also, note the increase in the $\mathbf{R_{eff}}$ predicted by the MGW model when $\mathbf{K_{min}}$ is smaller than $\mathbf{K_R}$ (as seen on the $\mathbf{R = -0.4}$ and part of the $\mathbf{R = 0.2}$ curves).

Another variation of the Generalized Willenborg model to account for reduction in retardation due to underloads is the ***Walker-Chang Willenborg*** (WCW) model, developed by Chang and Engle (1984). The WCW model applies the GW model to Walker-Chang's **da/dN** equation (Chang et al., 1984), and introduces an effective overload plastic zone $\mathbf{(Z_{ol})_{eff}}$, similar to Eq. (10), to model reduction in crack retardation. A limitation of the WCW model is that the reduction of the retardation effect is only accounted for an underload ***immediately*** following the tensile overload.

However, even with all proposed modifications to improve the original Willenborg model, the assumption regarding the residual compressive stresses through the residual stress intensity $\mathbf{K_{RW}}$ is still very doubtful (Broek, 1988). To better model the closure effects on crack retardation, some methods ***directly*** estimate the value of the opening stress intensity factor $\mathbf{K_{op}}$, instead of indirectly accounting for its effects through arbitrary parameters such as $\mathbf{K_{RW}}$. These $\mathbf{K_{op}}$ load interaction models are presented next.

3.4. $\mathbf{K_{op}}$ interaction models

In the $\mathbf{K_{op}}$ models, the opening stress intensity factor $\mathbf{K_{op}}$ caused by an overload is directly computed and applied to the ***subsequent*** crack growth to account for Elber-type crack closure. Perhaps the simplest $\mathbf{K_{op}}$ model is the ***Constant Closure*** model, developed at Northrop for use on their classified programs (Bunch et al., 1996). This model is based on the observation that for some load spectra the closure stress does not deviate substantially from a certain stabilized value. This stabilized value is determined by assuming that the spectrum has a "controlling overload" and a "controlling underload" that occur often enough to keep the residual stresses constant, and thus the closure level constant.

In the constant closure model, the opening stress intensity factor $\mathbf{K_{op}}$ is the only empirical parameter, with estimates between 30% and 50% of the maximum overload stress intensity factor. The crack opening stress $\mathbf{K_{op}}$ can also be calculated, for instance, from Newman's closure function in Eqs. (4-5), using the stress ratio **R** between the controlling underload and overload stresses. The calculated value of $\mathbf{K_{op}}$ is then applied to the following (smaller) loads to compute crack growth, recognizing crack retardation and crack arrest (if $\mathbf{K_{max} \leq K_{op}}$).

The main limitation of the Constant Closure model is that it can only be applied to loading histories with "frequent controlling overloads", because it does ***not*** model the ***decreasing*** retardation effects as the crack tip cuts through the overload plastic zone, as shown in Eqs. (7) and (12) for the Wheeler and Willenborg models. In the Constant Closure model, it is assumed that a new overload zone, with primary plasticity, is formed often enough before the crack can significantly propagate through the previous plastic zone, thus not modeling secondary plasticity effects.

To account for crack retardation due to **both** primary and secondary plasticity, the European Space Agency and the National Aerospace Laboratory in the Netherlands, in cooperation with the NASA Langley Research Center and the NASA Johnson Space Center, developed the ***DeKoning-Newman Strip Yield*** load interaction model (De Koning et al., 1997). In this model, a crack growth law is described in an ***incremental*** way, modeling crack growth attributed to increments $\boldsymbol{\delta}\mathbf{K}$ in the stress intensity factor as the crack changes from closed to fully open configurations. This incremental law is then integrated ***at each cycle*** from the minimum to the maximum applied stress intensity factors $\mathbf{K_{min}}$ and $\mathbf{K_{max}}$ to find the crack growth rate **da/dN**.

This incremental description allows that a distinction be made between the part of a load range where secondary plastic flow is observed and the part where primary plastic flow starts developing under a monotonic increasing load. For each of these domains, a different incremental crack growth law can be formulated. In DeKoning-Newman's Strip Yield model, four different loading regimens are considered as the crack is loaded from closed to fully open configurations: (i) *closed crack regime*, where the crack tip is at least partly closed, and no crack growth is assumed; (ii) *opened crack but no growth regime*, where the crack is fully opened, but only crack tip blunting without crack growth is observed; (iii) *fatigue crack growth regime*, where an incremental form of Elber's law is used to compute crack growth under secondary plastic flow; and (iv) *quasi-static crack extension regime*, where an incremental form of Paris' law is used to compute crack growth under primary plastic flow (insensitive to $\mathbf{K_{op}}$ or any other threshold behavior).

Using this model, it is possible to effectively calculate fatigue crack growth considering retardation and arrest due to ***both*** primary and secondary plasticity. The penalty of DeKoning-Newman's approach is the large number of experimental constants required by its crack propagation law, in addition to the numerical effort.

There are several other load interaction models in the literature (Suresh, 1998), but none of them has definitive advantages over the models discussed above. This is no surprise, since single equations are too simplistic to model all the several mechanisms that can induce retardation effects. Therefore, in the same way that a curve **da/dN** vs. **ΔK** must be experimentally measured, a load interaction model must be adjusted to experimental data to calibrate its parameters, as recommended by Broek (1988).

4. Comparison of the load interaction models

The load interaction models presented in this work have been implemented in `ViDa`, a powerful software developed to automate the fatigue dimensioning process by ***all*** the traditional methods used in mechanical design (Meggiolaro et al., 1998; Castro et al., 2000; Miranda et al., 2000). This software has been developed to predict ***both*** initiation and propagation fatigue lives under complex loading by ***all*** classical design methods: **SN**, **IIW** (for welded structures) and **εN** to predict crack initiation, and **da/dN** for studying plane and 2D crack propagation, ***considering*** load sequence effects. In this section, the presented load interaction models and the proposed modifications are compared with experimental results from various load spectra.

Using `ViDa`, the crack propagation life of an 8-mm-thick center-cracked tensile specimen, made of a 7475-T7351 aluminum alloy, is calculated using several block loading histories, see Tab. (1). The calculated lives are compared to experimental tests performed by Zhang (1987), who measured crack growth rates through scanning electron microscopy. Forman's crack growth equation (Forman et al., 1992) and Eq. (3) are used to compute crack growth (in mm), using $\mathbf{A = 6.9 \cdot 10^{-7}}$, **m = 2.212**, **p = 0.5**, **q = 1.0**, $\mathbf{\Delta K_0 = 3MPa\sqrt{m}}$, and $\mathbf{K_C = 73MPa\sqrt{m}}$. All models are calibrated using the first loading history (except for the Willenborg model, without parameters to be adjusted), and a comparison is made through the remaining loadings. Table (1) shows Zhang's test results and the percentage error of the predicted lives using several load interaction models.

Table 1. Percentage errors in the test lives predicted by the load interaction models.

Loading history	Zhang's test life (cycles)	No Interaction	Wheeler	Generalized Wheeler	Willenborg	Generalized Willenborg	Modif. Gen. Willenborg	Constant Closure
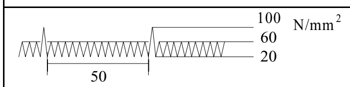	474,240	–17%	0%	0%	+293%	0%	0%	0%
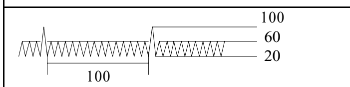	637,730	–36%	–22%	–22%	+269%	–22%	–22%	–22%
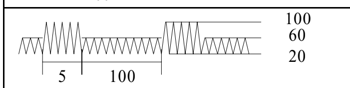	409,620	–13%	+2.3%	+2.3%	+185%	+2.2%	+2.6%	+2.4%
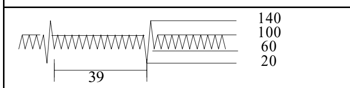	251,050	–27%	–18%	–18%	+27%	–20%	+24%	–75%
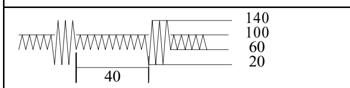	149,890	–2.3%	+6.6%	+6.4%	+44%	+4.0%	+42%	–60%

As expected, the Willenborg model resulted in poor predictions, since this model cannot be calibrated. The remaining models performed similarly for the second and third histories. However, as the maximum load increased from 100 to 140 MPa in the last two histories, the Modified Generalized Willenborg and the Constant Closure models showed increased errors. The Wheeler and Generalized Wheeler models performed very similarly, because the considered histories didn't include compressive underloads. These two models and the Generalized Willenborg model resulted in the best predictions for Zhang's histories. Unfortunately, these tests were performed under the second crack growth regimen (not influenced by the threshold $\mathbf{\Delta K_{th}}$), so the advantages of the Modified and Generalized Wheeler in modeling crack arrest were not exemplified above.

To compare the predictions of the load interaction models in the presence of underloads, an underload event $\mathbf{S_{ul}}$ was introduced after each overload of Zhang's second loading history, see Tab. (2).

Table 2. Comparison of life predictions in cycles for different underload stresses.

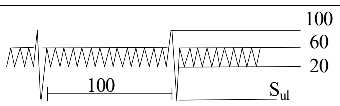

Underload stress $\mathbf{S_{ul}}$ (MPa)	Wheeler	Modified Wheeler	Generalized Wheeler	Generalized Willenborg	Modif. Gener. Willenborg	Constant Closure
20.0	497,100	496,900	496,900	497,650	499,350	497,100
0.0	493,700	493,600	493,600	494,500	457,850	495,700
–20.0	491,600	491,350	470,850	492,350	444,300	494,600
–50.0	488,200	487,950	427,750	488,950	433,000	492,350

As expected, the Generalized Wheeler and the Modified Generalized Willenborg were the only load interaction models that predicted reduction in retardation (and thus reduced life) after compressive underloads. The other models showed a slight reduction in the calculated lives in the presence of underloads, however this small change was caused only by the increased $\mathbf{\Delta K}$ ***at*** (and not ***after***) the overload/underload event.

Finally, to compare the performance of the several models under the first crack growth regimen (near the threshold $\mathbf{\Delta K_{th}}$), decreasing values of the initial crack $\mathbf{2a_0}$ are considered in Zhang's second loading history. Table (3) compares the lives predicted by the main load interaction models with the Generalized Wheeler predictions, using the calibrated parameters from Zhang's test results. Note that here the Modified Wheeler predictions are identical to the Generalized Wheeler ones, since the history below does not contain underload events.

Table 3. Comparison of life predictions for decreasing initial crack sizes.

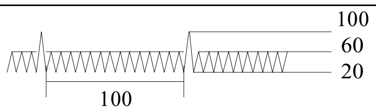

Initial crack size $\mathbf{2a_0}$ (mm)	Generalized Wheeler prediction (cycles)	Wheeler	Willenborg	Generalized Willenborg	Modif. Gener. Willenborg	Constant Closure
20.0	496,900	0.0%	+373%	+0.2%	+0.5%	0.0%
10.0	966,000	–0.7%	+406%	–3.6%	–0.2%	+0.1%
4.0	1,890,500	–3.1%	+920%	–10%	–0.4%	+0.1%
2.0	8,295,900	–47%	+313%	–67%	+8.1%	+0.2%

Except for the Willenborg model, all load interaction models predicted roughly the same fatigue life for $\mathbf{2a_0}$ = **20mm**. However, as the initial crack size was decreased, the influence of the threshold $\mathbf{\Delta K_{th}}$ was magnified. In fact, when $\mathbf{2a_0}$ = **2.0mm** the closure effects caused crack arrest (stop) between overloads during most of the specimen life, which was only captured by the Generalized (and the Modified) Wheeler and the Constant Closure models. The Generalized Willenborg model was too conservative, not predicting crack arrest in this case, because it requires that $\mathbf{K_{ol,max}}$ (100MPa in this history) be ***at least*** twice $\mathbf{K_{max}}$ (60MPa) to stop the crack, independently of $\mathbf{\Delta K_{th}}$. Even though the Modified Generalized Willenborg didn't capture crack arrest in this case either, its predictions were surprisingly close to the Generalized Wheeler and Constant Closure ones.

However, as seen in Tab. (1), both Modified Generalized Willenborg and Constant Closure models ***only*** resulted in good predictions when the 100MPa overload level (used in their calibration) was maintained. Furthermore, as discussed before, the Constant Closure model could only be successfully applied because all Zhang's histories have ***frequent*** controlling overloads (100 or 140MPa). In summary, the Generalized Wheeler model was the only one that performed well at both overload levels, while considering crack acceleration due to underloads and crack arrest. A qualitative comparison of the load interaction models, showing their main advantages and disadvantages, is presented in Tab. (4).

Table 4. Qualitative comparison of the load interaction models.

	da/dN	ΔK models		R_{eff} models				K_{op} models	
	Wheeler	Modified Wheeler	Generalized Wheeler	Willenborg	Generalized Willenborg	Modif. Gen. Willenborg	Walk.Chang Willenborg	Constant Closure	Strip Yield
models crack retardation	√	√	√	√	√	√	√	√	√
models crack arrest		√	√	√	√	√	√	√	√
models crack acceleration			√			√	√	√	√
works for any load spectrum	√	√	√	√	√	√	√		√
works with any da/dN equation	√	√	√					√	
models primary plasticity		√	√						√
number of experimental parameters	1	1	1-2	0	1	1	1-2	1	5

5. Conclusions

In this work, load interaction effects on fatigue crack propagation were discussed. Overload-induced retardation effects were evaluated using several different models, and improvements to the traditional equations were proposed to recognize crack arrest and acceleration due to compressive underloads. The models were evaluated using a general-purpose fatigue design software named ViDa. Using this software, the presented load interaction models and the proposed modifications were compared with experimental results for various load spectra. In particular, the proposed modifications to the Wheeler model showed an excellent agreement with the experimental data.

6. References

Broek, D., 1988, The Practical Use of Fracture Mechanics," Kluwer.

Bunch, J.O., Trammell, R.T., Tanouye, P.A., 1996, "Structural life analysis methods used on the B-2 bomber," *Advances in fatigue lifetime predictive techniques: 3rd Volume*, (A96-26758 06-39), ASTM, pp. 220-247.

Castro, J.T.P., Parks, D.M., 1982, "Decrease in Closure and Delay of Fatigue Crack Growth in Plane Strain," *Scripta Metallurgica*, Vol.16, pp.1443-1445.

Castro, J.T.P., Meggiolaro, M.A., 2000, "Automation of the Fatigue Design Under Complex Loading", I Seminário Internacional de Fadiga (SAE-Brasil), SAE #2000-01-3334, São Paulo, SAE.

Castro, J.T.P., Meggiolaro, M.A., 2001, "Fatigue Design under Complex Loading" (in Portuguese), PUC.

Chang, J.B., Engle, R.M., 1984, "Improved Damage-Tolerance Analysis Methodology," J.Aircraft, Vol.21, pp.722-730.

De Koning, A.U., Ten Hoeve, H.J., Hendriksen, T.K., 1997, "The description of crack growth on the basis of the strip-yield model for computation of crack opening loads, the crack tip stretch and strain rates," NLR-TP-97511L, NLR.

Elber, W., 1971, "The Significance of Fatigue Crack Closure," ASTM STP 486.

Forman, R. G., Mettu, S. R., 1992, "Behavior of Surface and Comer Cracks Subjected to Tensile and Bending Loads in Ti-6AI-4V Alloy," Fracture Mechanics: 22nd Symposium, Vol. I, ASTM STP 1131, pp. 519-546.

Gallagher. J.P., 1974, "A Generalized Development of Yield Zone Models," AFFDL-TM-74-28-FBR, Wright Patterson Air Force Laboratory.

Meggiolaro, M.A., Castro, J.T.P., 1997, "Modelagem dos Efeitos de Sequência na Propagação de Trincas por Fadiga", *2º Congresso Internacional de Tecnologia Metalúrgica e de Materiais*, ABM.

Meggiolaro, M.A., Castro, J.T.P., 1998, "ViDa - Danômetro Visual para Automatizar o Projeto à Fadiga sob Carregamentos Complexos," Brazilian Journal of Mechanical Sciences, Vol. 20, No. 4, pp.666-685.

Miranda, A.C.O., Meggiolaro, M.A., Castro, J.T.P., Martha, L.F. and Bittencourt, T. N., 2000, "Fatigue Crack Propagation under Complex Loading in Arbitrary 2D Geometries", *Applications of Automation Technology in Fatigue and Fracture Testing and Analysis: Fourth Volume, ASTM STP 1411*, ASTM, West Conshohocken, PA.

Newman, Jr., J. C., 1984, "A Crack Opening Stress Equation for Fatigue Crack Growth," International Journal of Fracture, Vol. 24, No. 3, pp. R131-R135.

Sippel, K.O., Weisgerber, D., 1977, "Flight by Flight Crack Propagation Test Results with Several Load Spectra and Comparison with Calculation According to Different Models," ICAF Symposium, Darmstadt.

Suresh, S., 1998, "Fatigue of Materials," Cambridge.

Von Euw,E.F.G., Hertzberg,R.W., Roberts,R., 1972, "Delay Effects in Fatigue Crack Propagation", ASTM STP 513.

Wheeler, O.E., 1972, "Spectrum Loading and Crack Growth," Journal of Basic Engineering, pp.181-186.

Willenborg, J., Engle, R.M., Wood, H.A., 1971, "Crack Growth Retardation Model Using an Effective Stress Concept," Air Force Flight Dynamics Laboratory, Wreight Patterson Air Force Base, Ohio, TM 71-1-FBR.

Zhang, S., Marissen, R., Schulte, K., Trautmann, K., Nowack, H., 1987, "Crack propagation studies on Al 7475 on the basis of constant amplitude and selective variable amplitude loading histories," Fatigue and Fracture of Engineering Materials and Structures, Vol. 10, No. 4, pp. 315-332.